Investigating the Therapeutic Potential of Lepidium sativum-Derived Compounds in Prostate Cancer: An Integrative in Silico Approach

Said Bitam

bitam.said@univ-medea.dz

Laboratory of Biomaterials and Transport Phenomena (LBMPT), University of Médéa

Mabrouk Hamadache

Laboratory of Biomaterials and Transport Phenomena (LBMPT), University of Médéa

Salah Hanini

Laboratory of Biomaterials and Transport Phenomena (LBMPT), University of Médéa

Research Article

Keywords: Lepidium sativum, Prostate cancer, Network pharmacology, molecular dynamics

Posted Date: October 20th, 2025

DOI: https://doi.org/10.21203/rs.3.rs-7302675/v1

Additional Declarations: No competing interests reported.

Version of Record: A version of this preprint was published at In Silico Pharmacology on November 6th, 2025. See the published version at https://doi.org/10.1007/s40203-025-00482-7.

Investigating the Therapeutic Potential of Lepidium sativum-Derived Compounds in Prostate Cancer: An Integrative in Silico Approach

Said Bitam[1*], Mabrouk Hamadache[1†] and Salah Hanini[1†]

[1*]Faculty of Technology, Department of Process Engineering and Environment, Laboratory of Biomaterials and Transport Phenomena (LBMPT), University of Médéa, :Médéa, Algeria.

*Corresponding author(s). E-mail(s): bitam.said@univ-medea.dz;
Contributing authors: hamadache.mabrouk@univ-medea.dz;
hanini.salah@univ-medea.dz;
†These authors contributed equally to this work.

Abstract

This study investigates the therapeutic potential of bioactive compounds from Lepidium sativum in the treatment of prostate cancer. Through of in silico analyses, three key compounds were identified and evaluated for their drug-likeness, pharmacokinetic properties, and safety profiles. These compounds demonstrated favorable drug-likeness according to Lipinski's rules and other drug-likeness criteria, high gastrointestinal tract absorption, and non-inhibition of major Cytochromes P450 enzymes. Protein-protein interaction network analysis identified ten hub genes, with AKT1 and PIK3CA emerging as prime targets for therapeutic intervention. Functional annotation and pathway analysis highlighted key biological processes and pathways associated with prostate cancer, emphasizing the significance of these targets. Molecular docking and dynamic simulation studies further confirmed the binding affinities and stability of the identified compounds with both mutated and non-mutated forms of the target genes. These findings suggest that compounds from Lepidium sativum hold promise as potential therapeutics for prostate cancer, warranting further investigation and development.

Keywords: Lepidium sativum, Prostate cancer, Network pharmacology, molecular dynamics

1 Introduction

Cancer remains a global health challenge, with breast, cervical, prostate, colorectal, and liver cancers collectively comprising nearly half of all new cancer cases worldwide [1]. Notably, prostate cancer (PC) stands out as the predominant malignancy in over fifty percent of countries globally, highlighting its substantial impact on global health [2]. Africa faces a significant battle against cancer, with approximately 1.1 million new cases reported annually, resulting in about 700,000 deaths [1]. Projections suggest a concerning increase in cancer-related mortality, with estimates nearing one million deaths per year by 2030, underscoring the urgent need for proactive interventions. Despite the prevalence of cancer, there is some optimism regarding the typically slow-growing nature of certain cancers, characterized by low-grade features and limited aggressiveness [3]. However, this positive outlook is tempered by the challenge of early detection, particularly evident in prostate cancer, which often manifests without discernible symptoms in its initial stages. Research on the correlation between dietary choices and cancer risk has garnered significant attention, with certain dietary factors demonstrating preventive properties against cancer while others may elevate the risk. Recent studies have shed light on the potential anticancer effects of various plant extracts, offering promising avenues for exploration [4, 5]. For instance, [6, 7] conducted a review on plant-derived bioactive compounds capable of modulating the growth of prostate cancer cells, highlighting their potential therapeutic alternatives for prostate cancer prevention and treatment. Additionally, a study by [8] provided supportive evidence indicating that increased consumption of healthful plant-based foods is associated with a reduced risk of aggressive forms of prostate cancer, with a more pronounced benefit observed among men aged under 65 years. Lepidium sativum, a member of the Cruciferae or Brassicaceae family, has garnered attention for its diverse array of effects, including antimicrobial, hypoglycemic, and anti-inflammatory properties [9]. While some studies have demonstrated the efficacy of Lepidium sativum and its active compounds in treating prostate cancer [10], it has also been traditionally used as a medicinal herb for prostate cancer treatment [11]. However, there remains a gap in silico studies exploring the potential of Lepidium sativum in prostate cancer treatment. Therefore, our study aims to elucidate the underlying mechanism of action of Lepidium sativum against prostate cancer. We will collect its bioactive components and employ a combination of network pharmacology, molecular docking approaches, and molecular dynamics simulations to identify novel protein targets for treatment.

2 Materials and methods

2.1 Screening of active compounds

Three hundred and ninety-eight compounds extracted from Lepidium sativum were obtained from PubChem (https://pubchem.ncbi.nlm.nih.gov/). The canonical simplified molecular-input line-entry system (SMILES) of these compounds was used to evaluate their drug-likeness and pharmacokinetics. The SMILES representations underwent analysis via the Swiss ADME web server (http://www.swissadme.ch/), assessing Lipinski's rule of 5, Ghose, Veber, Egan, and Muegge violations, along with

various pharmacokinetic properties including gastrointestinal absorption, blood-brain barrier permeability, CytochromeP450 inhibition, and p-glycoprotein substrate status. We used the ProTox-III webserver [12, 13], to predict the toxicity of these compounds, which ultimately led to the selection of three biologically active compounds biologically active compounds (**Supplementary File.S1**), were identified as potential bioactive ingredients of Lepidium sativum and chosen for further investigation. The 2D structures of these bioactive constituents were depicted using ChemDraw Ultra version 14.0 [14]. Sample body text. Sample body text. Sample body text. Sample body text. Sample body text. Sample body text. Sample body text.

2.2 Screening of potential target genes

The molecular structures of the seven Lepidium sativum compounds were submitted to Swiss Target Prediction [15], PharmMapper [16–18] and SuperPred [19] to obtain their target predictions. Only human (Homo sapiens) target proteins were included in the data retrieval, using UniProt ID to align the protein ID [20, 21]. Three thresholds were applied to select the most significant targets: a Z-score of ≥ 0.5 for PharmMapper, absolute values of scores (probabilities) of ≥ 0.1 for Swiss Target Prediction [22] and the probability that the input structure binds with the specific target of $\geq 70\%$ for SuperPred . After removing duplicated genes, a total of 266 targets were identified (**Supplementary File.S2**). A total of 8951 prostate cancer targets were retrieved from the GeneCards database [23], with the search limited to "prostate cancer", 4388 targets from DisgeNet [24] with the search limited to Name: Prostate carcinoma; CUI: C0600139, and 690 targets from Comparative Toxicogenomics Database (CTD) [25], with the search limited to "prostate cancer". A Venn diagram was utilized to identify the common intersection between prostate cancer-related targets and Lepidium sativum compounds targets. The diagram was generated using the online tool (https://www.interactivenn.net/). The genes that overlapped in this analysis were then used for further investigation.

2.3 Analysis of protein–protein interaction (PPI)

The intersecting target genes were analyzed using STRING Version 12.0 (https://string-db.org/) [26]. This database provides information on protein-protein interactions (PPI), including both known and predicted interactions, thereby offering insights into direct and indirect protein interactions. The analysis was conducted using "Homo sapiens" as the species, with a Confidence score threshold of 0.400 (medium confidence) to select targets for further investigation. The resulting PPI network was constructed and visualized using Cytoscape V 3.10.1 [27]. Data from the STRING database were imported into Cytoscape for analysis, and the Cytohubba plugin [28] was used to identify the top 10 interacting genes based on degree centrality.

2.4 Functional annotation and pathway analysis

Gene Ontology (GO) and Kyoto Encyclopedia of Genes and Genomes (KEGG) pathway enrichment analyses were performed to elucidate the fundamental mechanisms

and pathways associated with all potential targets. Functional annotation and pathway analysis were conducted using the Database for Annotation, Visualization and Integrated Discovery (DAVID; https://david.ncifcrf.gov/) [29]. The common targets identified from the Venn diagram were analyzed using DAVID web server, with "Homo sapiens" selected as the species to predict gene functions across three levels: Molecular function (MF), Biological process (BP), and Cellular component (CC), in addition to KEGG (Kyoto Encyclopaedia of Genes and Genomes) pathways. KEGG pathway analysis aids in comprehending the overarching functions and processes within biological systems. In this study, significance was determined by a p-value of ≤ 0.05, and the top 10 GO enrichment terms and KEGG pathways with the highest counts were selected for further investigation.

2.5 Therapeutic potential of hub genes

The common targets identified from the Venn diagram analysis were investigated using the Open Targets Platform (http://www.targetvalidation.org). This platform allows users to input query gene IDs and provides output including the overall Association Score, predicted tractability (such as small molecule inhibitors and antibodies), and known drug information (target diseases, mode of action, clinical trials, etc.) associated with the queried gene.

2.6 Mutation analysis

The mutation rates of the prostate cancer targets influenced by Lepidium sativum compounds were retrieved from the extensive database Cbioportal (http://www.cbioportal.org). Our data originated from the Prostate Adenocarcinoma (MSK, Clin Cancer Res. 2022) dataset [30], which comprises a substantial collection of 1417 samples. By inputting the gene ID and cancer type, the oncoprint feature available on this web server visualizes the genetic alterations of the queried genes through heatmaps with z-score values. Additionally, the mutation pattern of hub gene pairs in prostate cancers is calculated using Log_2 Odds Ratio (OR).

2.7 Expression analysis of hub genes

The expression levels of the queried hub genes were analyzed in both normal and cancerous tissues using the GEPIA2 web server (http://gepia2.cancer-pku.cn/). Genes exhibiting a $|\log_2 \text{fold change}| \geq 1$ were regarded as statistically significant at a p-value of ¡0.01. Furthermore, the correlation between the expression status of hub genes and disease-free survival was investigated. This involved examining the relationship between gene expression profiles in prostate cancer (PC) and normal tissues using a log-rank test, with statistical significance set at $p < 0.05$.

2.8 Molecular docking analysis

Molecular docking was employed to elucidate the interactions between the core targets and active compounds. The 3D structures of the selected targets, including both native (wild-type) and mutant forms of AKT1 (PDB IDs: 4GV1 and 3QKM) and PIK3CA

(PDB IDs: 4L23 and 4JPS), were retrieved from the RCSB Protein Data Bank (PDB) in PDB format (https://www.rcsb.org/). The initial steps involved preparing the protein structure by eliminating surrounding water molecules near the protein. Grid coordinates associated with co-crystallized ligands were recorded, and the existing ligand was removed to clear the active site. Gasteiger charges were computed, and polar hydrogen atoms were added, while non-polar hydrogen atoms were merged, maintaining the protein structure's rigidity. Conversely, the ligand was allowed to be flexible, enabling the exploration of the most favorable binding conformation through the rotation of its rotatable bonds. Molecular docking of core targets and active compounds was conducted using Autodock Vina software. The docking grid parameters for AKT1 and PIK3CA are listed in **Supplementary File.S3**. Docking complexes with low root mean square deviation (RMSD) and low binding energy were prioritized for further analysis. The docking score served as a crucial evaluation criterion to filter out potential compounds and their respective targets, providing insights into the accuracy and strength of the protein-compound binding. Additionally, BIOVIA Discovery Studio Visualizer v24.1.0.23298 and the PLIP web server were utilized to visualize 2D and 3D interactions of docking complexes.

2.9 Molecular dynamics simulation

The optimal protein-ligand complexes structure obtained from molecular docking were subjected to further analysis through molecular dynamics simulations (MD) using GROMACS 2020. Ligand and protein parameters were generated using the CHARMM36 force field via the web-based CHARMM-GUI platform (https://charmm-gui.org/). The systems were solvated with transferable intermolecular potential water molecules (TIP3) within cubic periodic boundary conditions. To maintain system neutrality, sodium (Na^+) and chloride (Cl^-) counter-ions were added, ensuring an isosmotic condition of 0.15 M NaCl. MD simulations were conducted for 20 ns. The temperature was kept constant at 300.15 K during the NVT equilibration phase, while the NPT equilibration phase maintained a pressure of 1 bar. Various parameters were utilized to evaluate ligand-protein interactions. Hydrogen bonds were analyzed to assess the interactions between the ligand and the protein. The root mean square deviation (RMSD) of the protein was monitored to gauge its stability throughout the simulation. The radius of gyration (Rg) and the root mean square fluctuation (RMSF) of amino acid residues were also examined to understand the flexibility of the protein and its response to ligand binding.

3 Results and discussion

3.1 Screening of active compounds and target predictions

Fig.1 depicts the three compounds that were chosen. The drug-likeness of Lepidium sativum compounds was evaluated according to Lipinski's rules [31], alongside the Veber [32], Ghose [33], Egan [34], and Muegge [35] violations count for drug candidates. These compounds meet all specified criteria without violations: fewer than five hydrogen bond donors, fewer than 10 hydrogen bond acceptors, molecular weight

below 500 Da, and log P-value under five. The drug-likeness assessment results are summarized in **Table 1**. Since these compounds comply with Lipinski's Rule, they are considered potential orally bioavailable agents.

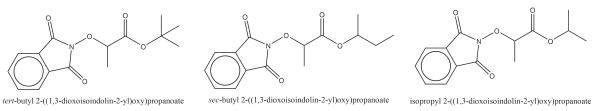

Fig. 1 2D structure of selected Lepidium sativum compounds.

The bioavailability radar plot (**Supplementary File.S4**) shows that these compounds fall within the optimal range (pink area), indicative of favorable drug-likeness. Additionally, they exhibit fewer than ten rotatable bonds, suggesting high oral bioavailability. The topological polar surface area (TPSA) [36] also supports good oral bioavailability (TPSA > 20 Å and < 130 Å).

Table 1 . ADME properties calculated for selected Lepidium sativum-Derived Compounds using SwissADME and ProTox-III webservers

Compounds	**Molecule 01**	**Molecule 02**	**Molecule 03**
MW	277.27	291.3	291.3
TPSA	72.91	72.91	72.91
WLOGP	1.17	1.56	1.56
GI absorption	High	High	High
BBB permeant	No	No	No
Pgp substrate	No	No	No
CYP1A2 inhibitor	No	No	No
CYP2C19 inhibitor	No	No	No
CYP2C9 inhibitor	No	No	No
CYP2D6 inhibitor	No	No	No
CYP3A4 inhibitor	No	No	No
Lipinski violations	0	0	0
Ghose violations	0	0	0
Veber violations	0	0	0
Egan violations	0	0	0
Muegge violations	0	0	0
Bioavailability Score	0.55	0.55	0.55
Hepatotoxicity	Inactive	Inactive	Inactive
Cardiotoxicity	Inactive	Inactive	Inactive
Carcinogenicity	Inactive	Inactive	Inactive
Immunotoxicity	Inactive	Inactive	Inactive
Mutagenicity	Inactive	Inactive	Inactive
Cytotoxicity	Inactive	Inactive	Inactive

The boiled egg graph (**Supplementary File.S4**), correlating TPSA and WLogP [37], further confirms these favorable attributes related to gastrointestinal absorption and lipophilicity. These compounds demonstrate high gastrointestinal tract absorption potential, positioning them as promising drug candidates. Notably, they

are not P-glycoprotein (P-gp) substrates, which enhances their suitability against multidrug-resistant cancer cells that overexpress this transporter [38]. Furthermore, their inability to permeate the blood-brain barrier suggests limited access to the brain's specific receptors. Predictions regarding potential drug-drug interactions through Cytochromes P450 (CYPs) inhibition indicate that these compounds are not inhibitors of CYP1A2, CYP2C19, CYP2C9, CYP2D6 and, CYP3A4 minimizing the risk of metabolic interference with other xenobiotics. These pharmacokinetic attributes underscore their potential for gastrointestinal absorption while averting blood-brain barrier penetration [39–41], positioning them as intriguing candidates for further pharmaceutical investigation. Furthermore, safety evaluation (**Table 1**) demonstrates that Lepidium sativum compounds exhibit a favorable safety profile, showing no hepatotoxicity [42] or other toxicological concerns such as carcinogenicity [43], immunotoxicity [44], mutagenicity [45], or cytotoxicity [46] . This safety profile enhances their potential for therapeutic applications.

3.2 Protein–protein interaction (PPI)

To construct the protein-protein interaction (PPI) network, we utilized the 34 genes identified from the Venn diagram in **Fig.2**, representing the common intersection, and submitted them to the STRING database.

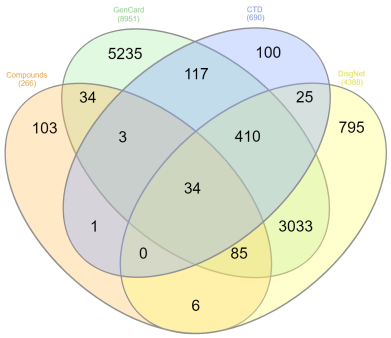

Fig. 2 Venn Diagram of Targets Identified from Lepidium sativum Compounds and Prostate Cancer.

This PPI network visually represents the interconnections among various target genes under disease conditions. The interactions and relationships between each gene are depicted using nodes and edges within the STRING database. **Fig.3a** displays the resulting PPI network of the 34 genes, analyzed using Cytoscape V 3.10.1, comprising 34 nodes and 126 edges. Node size corresponds to the degree centrality obtained from topology analysis. We employed the CytoHubba plugin to prioritize the top ten genes based on the degree method,as shown in **Fig.3b**. Nodes with the highest degrees are visually highlighted in red within the PPI network, while nodes with lower degrees are represented in yellow. Notably, the top-ranking genes within this network, based on their degree centrality, include MMP9, PPARA, AKT1, GSK3B, PIK3CA, ESR1,

MDM2, ESR2, STAT3, and SOD2. The genes ESR1, STAT3, AKT1, MMP9, MDM2, and GSK3B demonstrated the highest degree centrality within the network, signifying their significant and extensive interactions. Targeting these central nodes aimed to identify promising candidates for therapeutic intervention in prostate cancer research.

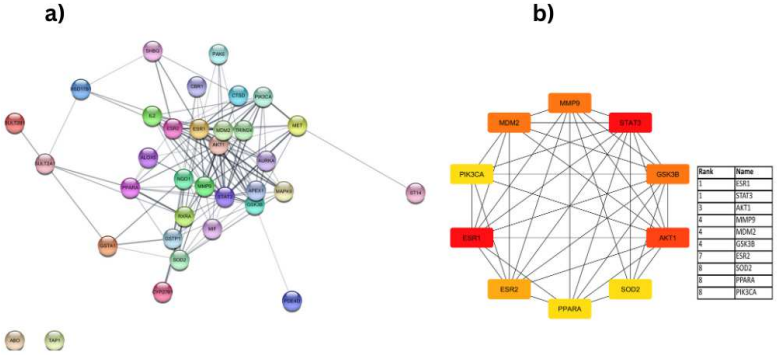

Fig. 3 a) PPI Network Resulting from the 34 Genes. b) Top Ten Genes Based on the Degree Method.

3.3 Functional annotation and pathway analysis

The potential biological functions of prostate cancer targets were investigated by analyzing their functional annotation and conducting enrichment analysis of hub genes selected from the protein-protein interaction (PPI) network. This analysis resulted in the enrichment of 65 biological processes (BP), 11 cellular components (CC), 26 molecular functions (MF), and 76 KEGG pathways. A bubble plot highlighting the top terms based on their p-value and counts was visualized (**Fig.4**). According to the Gene Ontology (GO) biological processes analysis, the prostate cancer targets were associated with processes such as negative regulation of gene expression, negative regulation of apoptosis, and positive regulation of DNA-templated transcription. The GO cellular component analysis revealed that the target genes were predominantly located in the cytosol, cytoplasm, and plasma membrane. In terms of GO molecular function analysis, the target genes were implicated in functions such as RNA polymerase II transcription factor activity, ligand-activated sequence-specific DNA binding, and enzyme binding. The KEGG pathway analysis highlighted significant signaling pathways associated with prostate cancer. Specifically, genes were found to be involved in pathways such as Cancer, Prolactin signaling, Endocrine resistance, Proteoglycans in cancer, Chemical carcinogenesis via receptor activation, Lipid metabolism, atherosclerosis, and notably, Prostate cancer (involving 5 genes: GSK3B, PIK3CA, MDM2, AKT1, MMP9).

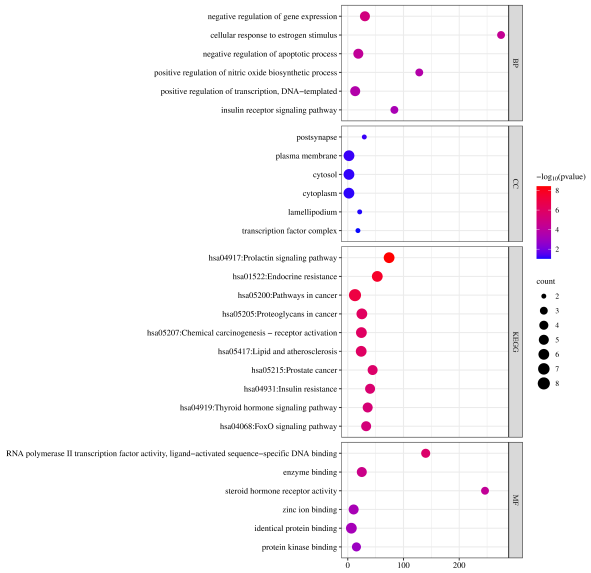

Fig. 4 Functional annotation and enriched pathways representation in the form of Bubble Plot: GO in terms of biological processes (BP), GO cellular components (CC), KEGG pathway analysis, and GO in terms of molecular function (MF).

3.4 Molecular tractability potential of hub genes

Based on the **Table 2**, the most favorable genes for therapeutic research are AKT1, PIK3CA, ESR1, and ESR2, as indicated by their high global scores and extensive tractability predictions. AKT1, with a global score of 0.627, is targeted by inhibitors such as IPATASERTIB, CAPIVASERTIB, MK-2206, and AFURESERTIB, spanning clinical phases I to III, and shows strong tractability predictions with small molecule clinical precedence rated at 5, antibody clinical precedence at 2, and Protac at 5. PIK3CA, with a global score of 0.620, is targeted by inhibitors like BUPARLISIB, SAMOTOLISIB, SONOLISIB, APITOLISIB, DACTOLISIB, and COPANLISIB, in clinical phases I and II. It also demonstrates high tractability with a small molecule clinical precedence of 5, antibody clinical precedence of 1, and Protac at 4. ESR1 has a global score of 0.558 and is targeted by agonists such as TAMOXIFEN CITRATE, FULVESTRAN, and ESTETROL, spanning clinical phases I to III, with excellent tractability predictions: small molecule clinical precedence at 5, antibody clinical precedence at 3, and Protac at 5. ESR2, with a global score of 0.485, is modulated by ESTRAMUSTINE PHOSPHATE SODIUM in phase III trials, and also shows high tractability with small molecule clinical precedence at 5, antibody clinical precedence at 3, and Protac at 5. These genes, highlighted by their higher global scores, indicate a strong association with diseases, and their diverse and advanced clinical tractability predictions make them promising targets for therapeutic research and development.

Understanding mutations is crucial for unraveling the mechanisms behind drug resistance in cancer cells. Analysis using the cBioPortal for Cancer Genomics revealed

Table 2 Key Information on 10 Genes and Their Disease Associations, Drug Actions, Clinical Trials, and Tractability Predictions

Gene	Global Score	Known drugs	Phase	Tractability predictions		
				Small molecule clinical precedence	Antibody clinical precedence	Protac
ESR2	0.485	ESTRAMUSTINE PHOSPHATE SODIUM	Phase III	5	3	5
STAT3	0.355	-	-	3	1	4
SOD2	0.014	-	-	1	-	3
PPARA	0.011	-	-	5	-	1
MMP9	0.082	-	-	5	4	2
AKT1	0.627	IPATASERTIB CAPIVASERTIB MK-2206	Phase III Phase III Phase II	5	2	5
GSK3B	0.259	AFURESERTIB LITHIUM CARBONATE	Phase I Phase I	5	2	4
PIK3CA	0.62	BUPARLISIB SAMOTOLISIB SONOLISIB APITOLISIB DACTOLISIB COPANLISIB	Phase II Phase II Phase II Phase I Phase I Phase I	5	1	4
ESR1	0.558	TAMOXIFEN CITRATE FULVESTRAN ESTETROL	Phase III Phase II Phase I	5	3	3
MDM2	0.444	-	-	5	1	4

that four genes showed no mutations among 1417 samples, while the remaining six genes exhibited various alterations, including frameshift, missense, splice, truncating mutations, structural variants, amplifications, and deep deletions (**Fig.5**). These genes showing molecular alterations in prostate cancer samples as follows;PIK3CA (4%), AKT1 (2%), STAT3 (1.4%), GSK3B (0.8%), MDM2 (0.8%), and ESR1 (0.5%). Given that these six genes are therapeutic targets in prostate cancer, mutations within them can lead to drug resistance. Mutations occurring within binding sites can decrease the affinity of drugs or compounds for their targets, underscoring the critical role of these genes in prostate cancer.

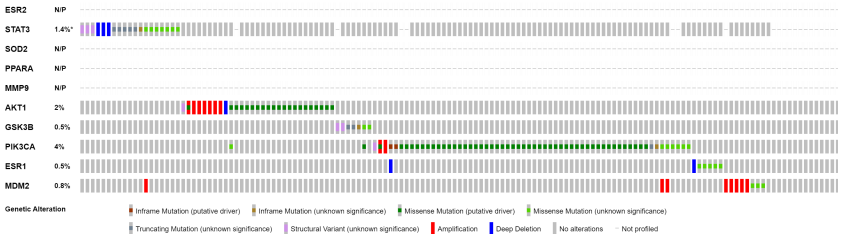

Fig. 5 Mutational Profile of Key Prostate Cancer Hub Genes

3.5 Gene expression

The analysis from GEPIA revealed notable expression changes among the 10 hub genes in prostate adenocarcinomas (PRAD). Specifically, AKT1, MMP9, and GSK3B exhibited upregulation, while MDM2 showed non-significant changes. On the other hand, STAT3, AKT1, ESR1, ESR2, PIK3CA, GSK3B, MMP9, SOD2, and PPARA were downregulated in PRAD (Prostate adenocarcinoma) compared to normal prostate tissues, with fold changes exceeding 1.5 ($p < 0.01$). These findings underscore the significant roles of these genes in the development of prostate cancer (**Fig.6**). Furthermore, Kaplan-Meier survival analysis revealed that none of the 10 hub genes exerted a positive impact on overall survival among prostate cancer patients.

3.6 Alignment examination

The Venn diagram in **Fig.7** illustrates an alignment examination of ten hub genes using various systems biology methods. Among the four functional prediction tools utilized, the genes AKT1 and PIK3CA were notably enriched. This enrichment was observed through KEGG pathway analysis, highlighting their potential suitability for targeting in prostate cancer. Additionally, these genes demonstrated significant text-mining scores, exhibited molecular alterations in prostate cancer samples, and showed either upregulation or downregulation in prostate adenocarcinoma, emphasizing their critical role in this disease. For these reasons, AKT1 and PIK3CA were selected for docking and further investigation.

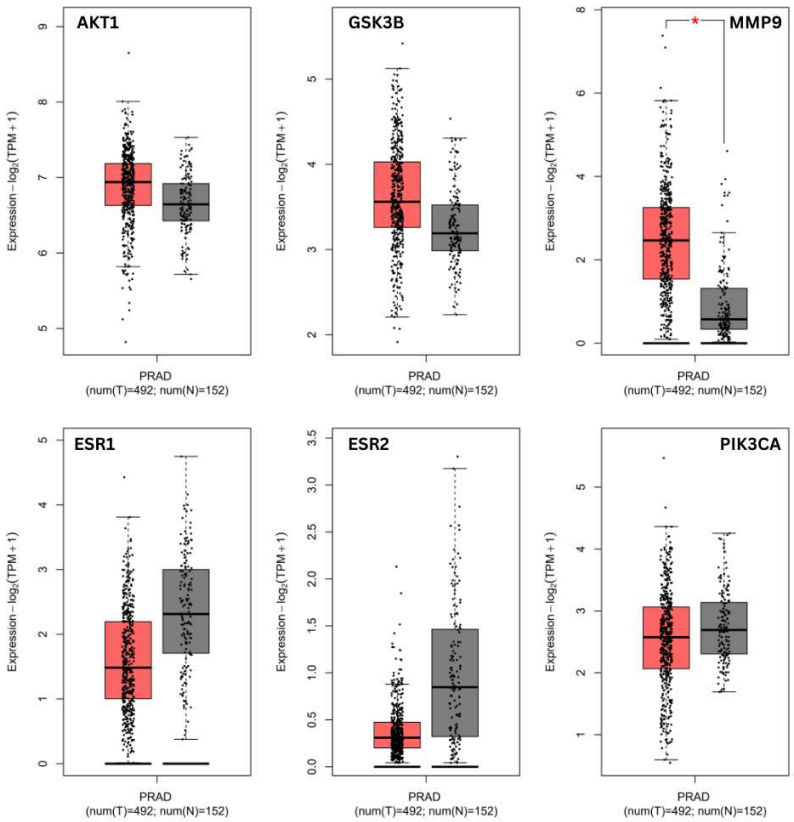

Fig. 6 Differential Gene Expression in Prostate Cancer Compared to Normal Tissues

3.7 Molecular docking analysis

Docking studies were conducted on both mutated and non-mutated forms of these targets using appropriate molecules, and the results are detailed in **Table 3**. The binding affinity of AKT1 and PIK3CA, whether mutated or non-mutated, with their respective molecules, is presented in this table. Additionally, **Fig.8** provide 3D docked structures of AKT1 and its interactions with the ligands. In the case of non-mutated genes, drugs listed in **Table 2** demonstrated favorable interactions with AKT1 during phase I trials, showing binding affinities ranging from −7.4 kcal/mol to −7.7 kcal/mol. Our study focused on phase I trials, as indicated in **Table 3**. Notably, many amino acids involved in the interactions observed during phase I of Afuresertib's interaction with 4GV1 (with a positive binding affinity of −8.7 kcal/mol) align with those identified in the docking of compounds 01, 02, and 03 (LEU:156A, VAL:164A, ALA:177A, PHE:438A, and THR:291A). Similarly, PIK3CA showed favorable interactions with selected drugs from **Table 2**, with binding affinities ranging from −6.8 to −7.0 kcal/-mol. Our analysis identified key amino acids (ILE:848A, ILE:932A, TYR:836A, and

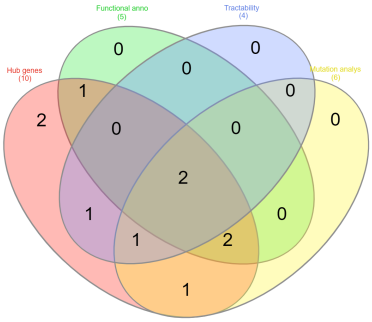

Fig. 7 Overlap of Key Prostate Cancer Hub Genes Identified by Different Systems Biology Approaches

ASP:933A) that interacted with a promising drug candidate (compound 01) similarly to a known drug (Dactolisib) during early (phase I) testing. Interestingly, these amino acids were also involved in the testing of other similar drugs (compounds 02 and 03). In contrast, other drugs (Copanlisib and Apitolisib) exhibited fewer interactions in early testing. These findings highlight compounds 01, 02, and 03 as candidates deserving further investigation in phase 1 trials for prostate cancer treatment. Regarding mutated genes, the binding affinities of mutated 3QKM with selected compounds ranged from −7.1 to −7.3 kcal/mol. Four amino acids involved in the interactions of Afuresertib with 3QKM align with those identified in the docking of compounds 01, 02, and 03 (LEU:156A, VAL:164A, ALA:177A, and PHE:438A). Similarly, PIK3CA demonstrated favorable interactions with selected drugs. Notably, interactions of the mutated gene 4JPS with Copanlisib, Dactolisib, and Apitolisib showed the highest binding affinities ranging from −8.0 to −10.0 kcal/mol. Three amino acids involved in the interactions of Copanlisib with 4JPS and Dactolisib with 4JPS corresponded with those identified in the docking of compounds 01, 02, and 03 (ILE:848A, ILE:932A, and TYR:836A). In the case of Apitolisib, three amino acids (ILE:800A, LEU:807A, and ILE:848A) were identified that are shared with those involved in the interactions observed during the docking of compounds 01, 02, and 03 with 4JPS. These findings underscore the potential significance of these drugs for further investigation in targeted therapies for mutated genes in prostate cancer.

3.8 Molecular Dynamic Simulation Analysis

In our study of molecular dynamics, we focused on investigating the interaction of Compound 03 and Afuresertib with both non-mutated (**Fig.9**) and mutated (**Fig.10**) forms of the gene AKT1. The molecular dynamics (MD) simulations provided a dynamic perspective on the structural stability and conformational changes of the protein-ligand complexes over time.

Table 3 The binding affinity of AKT1 and PIK3CA, whether mutated or non-mutated

Target	Mutation	Complex	Vina score	NHB	NHI	Other
AKT1	Non-mutated	4GV1-mol1	−7.4	1	8	none
		4GV1-mol2	−7.6	2	7	none
		4GV1-mol3	−7.7	2	6	none
PIK3CA	Non-mutated	4L23-mol1	−7	2	4	1 Salt Bridge + 1 π-Stacking
		4L23-mol2	−6.8	1	6	1 π-Stacking
		4L23-mol3	−6.8	1	6	1 π-Stacking
AKT1	Mutated	3QKM-mol1	−7.1	1	7	none
		3QKM-mol2	−7.1	0	8	none
		3QKM-mol3	−7.3	0	6	none
PIK3CA	Mutated	4JPS-mol1	−7.5	0	8	1 Salt Bridge + 2 π-Stacking
		4JPS-mol2	−7.7	0	10	1 Salt Bridge + 2 π-Stacking
		4JPS-mol3	−7.2	0	9	none
AKT1	Control drug - Phase I	4GV1_Afuresertib	−8.7	3	6	1 Halogen Bond
		3QKM_Afuresertib	−8.4	1	3	none
PIK3CA	Control drug - Phase I	4L23-Copanlisib	−7.4	4	3	none
		4L23-Dactolisib	−10.1	3	5	1 π-Stacking
		4L23-Apitolisib	−7.9	6	3	2 Salt Bridges
		4JPS-Copanlisib	−8	6	4	none
		4JPS-Dactolisib	−10	3	4	1 π-Stacking
		4JPS-Apitolisib	−9.4	4	6	none

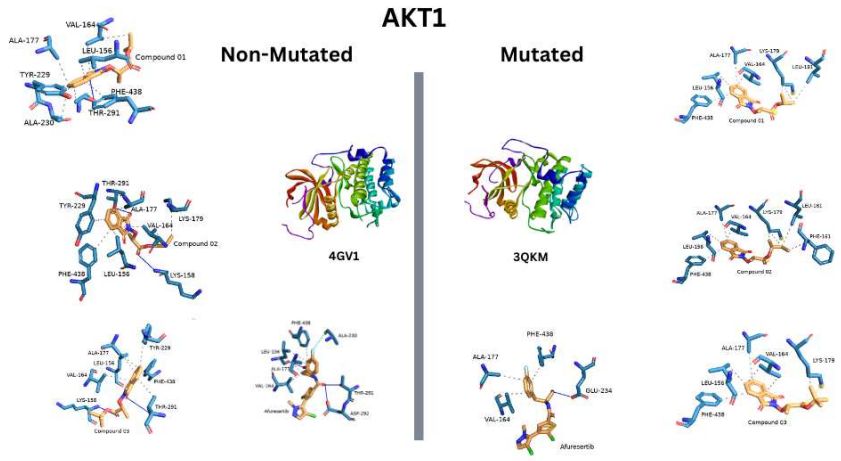

Fig. 8 3D Structural Interactions of Mutated and Non-mutated AKT1 with Ligands

3.8.1 Root-Mean-Square Deviation (RMSD) Analysis

The RMSD values for the 4GV1-Compound 03 complex exhibited higher fluctuations compared to the 4GV1-Afuresertib complex. This suggests that the Compound 03 complex is less structurally stable and experiences greater deviations from the initial binding pose over the simulation time. Similarly, the 3QKM-Compound 03 complex also showed larger RMSD values compared to the 3QKM-Afuresertib complex, indicating a less consistent molecular structure for the Compound 03 complex when bound to the mutated protein.

3.8.2 Root-Mean-Square Fluctuation (RMSF) Analysis

The RMSF analysis was conducted to assess the flexibility and mobility of the protein-ligand complexes. The 4GV1-Compound 03 complex displayed elevated RMSF values for several key amino acid residues compared to the 4GV1-Afuresertib complex. This suggests that the Compound 03 complex exhibits greater flexibility and potential instability in certain regions of the protein structure. A similar trend was observed for the 3QKM-Compound 03 complex, where increased RMSF values were observed for specific residues compared to the 3QKM-Afuresertib complex.

3.8.3 Hydrogen Bond Analysis

The formation and persistence of hydrogen bonds between the ligand and the protein are crucial for maintaining stable binding interactions. The MD simulations revealed that the 4GV1-Compound 03 complex formed fewer hydrogen bonds, and these bonds were less persistent over the simulation time, compared to the 4GV1-Afuresertib complex. This indicates a weaker network of hydrogen bonding interactions for the Compound 03 complex. The same pattern was observed for the 3QKM-Compound 03

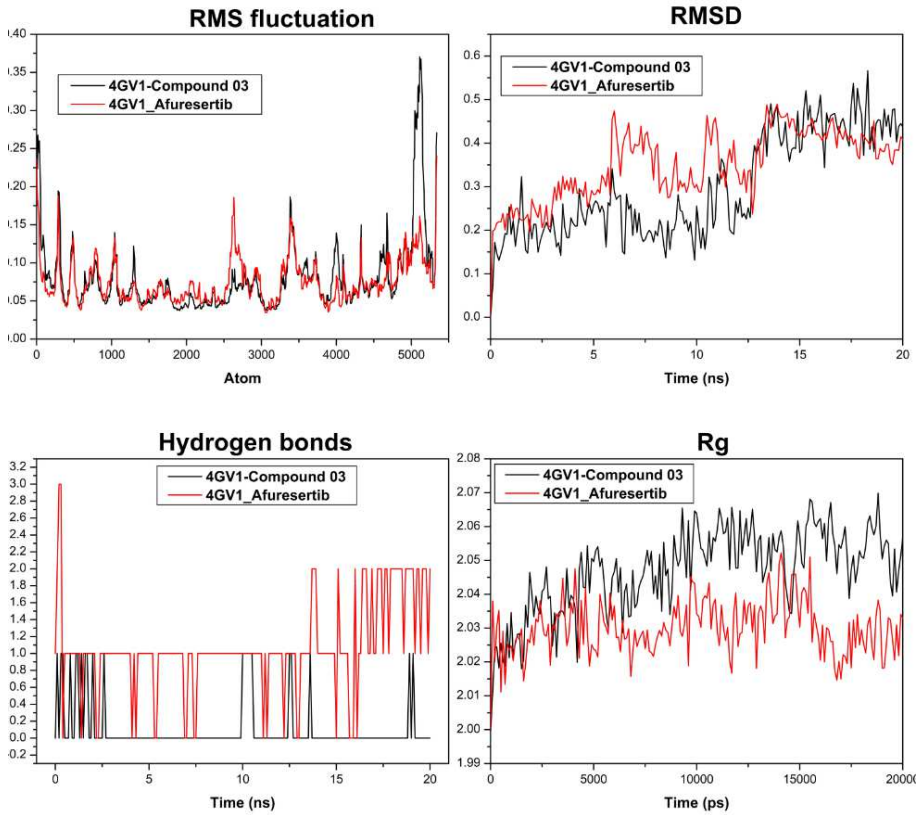

Fig. 9 Molecular Dynamics Simulation of Non-mutated AKT1 Interacting with Compound 03 and Afuresertib

complex, where fewer and less stable hydrogen bonds were formed compared to the 3QKM-Afuresertib complex.

3.8.4 Compactness Analysis

The compactness of the protein-ligand complexes was analyzed to assess the quality of the binding interactions. The 4GV1-Compound 03 complex exhibited a less compact molecular structure compared to the 4GV1-Afuresertib complex, suggesting potentially less favorable interactions. Similarly, the 3QKM-Compound 03 complex showed a less consistent and compact molecular structure compared to the 3QKM-Afuresertib complex. These findings from the MD simulations complement the insights gained from the earlier docking analysis. The docking study provided an initial assessment of the binding poses and interactions of Compound 03 with the 4GV1 and 3QKM protein targets, suggesting potential limitations in its binding affinity compared to Afuresertib. The detailed MD simulation analysis has now further highlighted the

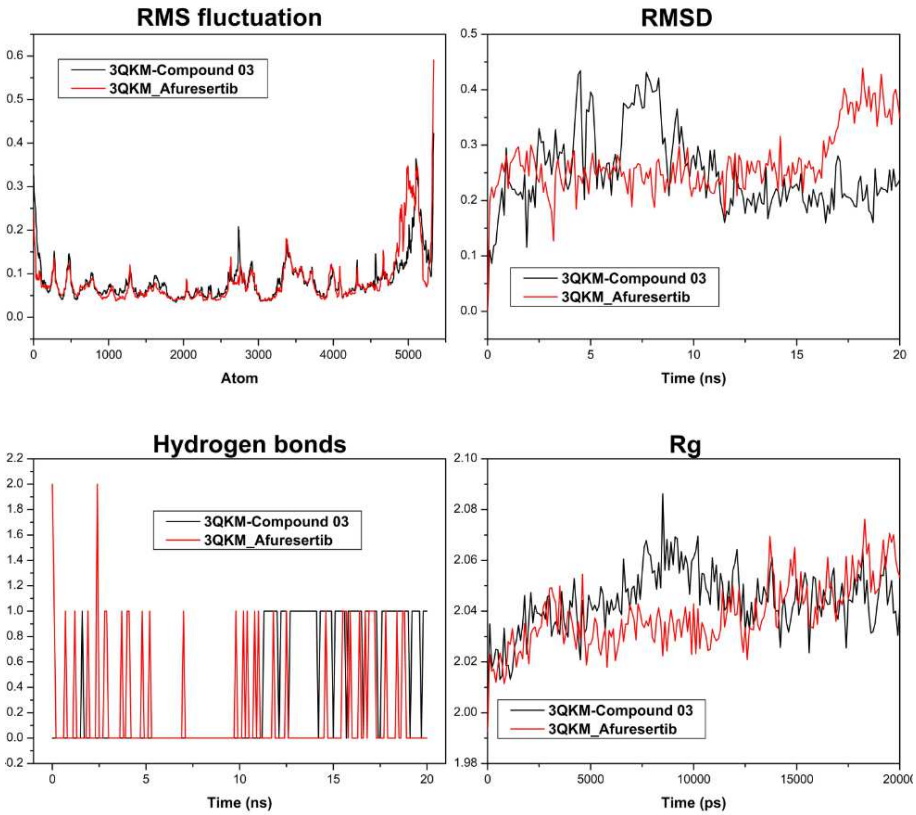

Fig. 10 Molecular Dynamics Simulation of Mutated AKT1 Interacting with Compound 03 and Afuresertib

dynamic stability and structural properties of the protein-ligand complexes, reinforcing the potential challenges faced by Compound 03 in maintaining consistent and favorable binding interactions. The combination of docking and MD simulation analyses provides a comprehensive understanding of the binding characteristics and structural dynamics of Compound 03 compared to the approved drug Afuresertib. These insights can help guide further optimization efforts and experimental validations to improve the therapeutic potential of Compound 03 for the treatment of prostate cancer.

4 Conclusion

Our comprehensive study highlights the significant potential of bioactive compounds derived from Lepidium sativum in targeting prostate cancer. Through rigorous screening, molecular docking, and dynamic simulations, we identified key compounds that exhibit strong binding affinities and stability with critical prostate cancer targets,

notably AKT1 and PIK3CA. The pharmacokinetic properties and safety profiles of these compounds further support their candidacy as therapeutic agents. While our findings are promising, further experimental validation and clinical trials are essential to confirm their efficacy and safety in vivo. This research underscores the value of integrating computational and experimental approaches in the discovery and development of novel cancer therapeutics.

Declarations

- **Funding**: This research did not receive any specific grant from funding agencies in the public, commercial, or not-for-profit sectors.

- **Competing interests**: The authors declare that they have no known competing financial interests or personal relationships that could have appeared to influence the work reported in this paper.
- **Ethics approval and consent to participate**: Not applicable. This study does not involve human participants or animal experiments.
- **Consent for publication**: Not applicable.
- **Data availability**: The datasets generated and/or analyzed during the current study are available from the corresponding author upon reasonable request.
- **Materials availability**: Not applicable.
- **Code availability**: Custom scripts used during the current study are available from the corresponding author upon reasonable request.

References

[1] Moeti, D.M.: World Cancer Day 2023 – Message of WHO Regional Director for Africa. https://www.afro.who.int/regional-director/speeches-messages/world-cancer-day-2023. Accessed 2024-02-03 (2023)

[2] Grossman, D.C., Curry, S.J., Owens, D.K., Bibbins-Domingo, K., Caughey, A.B., Davidson, K.W., Doubeni, C.A., Ebell, M., Epling, J.W., Kemper, A.R., *et al.*: Screening for prostate cancer: Us preventive services task force recommendation statement. J. Am. Med. Assoc. **319**(18), 1901–1913 (2018) https://doi.org/10.1001/jama.2018.3710

[3] Harvey, C., Pilcher, J., Richenberg, J., Patel, U., Frauscher, F.: Applications of transrectal ultrasound in prostate cancer. Br. J. Radiol. **85**(suppl_1), 3–17 (2012) https://doi.org/10.1259/bjr/56357549

[4] Ma, J., Peng, C.: Nigella sativa plant extract inhibits the proliferation of mda-mb-231 breast cancer cells via apoptosis and cell cycle arrest. Bangladesh J. Pharmacol. **19**(1), 29–38 (2024) https://doi.org/10.3329/bjp.v19i1.71069

[5] Raad, C., Raad, A., Pandey, S.: Green tea leaves and rosemary extracts selectively induce cell death in triple-negative breast cancer cells and cancer stem cells and

enhance the efficacy of common chemotherapeutics. Evid. Based Complement. Alternat. Med. **2024**(1), 9458716 (2024) https://doi.org/10.1155/2024/9458716

[6] Salehi, B., Fokou, P.V.T., Yamthe, L.R.T., Tali, B.T., Adetunji, C.O., Rahavian, A., Mudau, F.N., Martorell, M., Setzer, W.N., Rodrigues, C.F., *et al.*: Phytochemicals in prostate cancer: From bioactive molecules to upcoming therapeutic agents. Nutrients **11**(7), 1483 (2019) https://doi.org/10.3390/nu11071483

[7] Thomas-Charles, C., Fennell, H.: Anti-prostate cancer activity of plant-derived bioactive compounds: A review. Curr. Mol. Biol. Rep. **5**, 140–151 (2019) https://doi.org/10.1007/s40610-019-00123-x

[8] Loeb, S., Fu, B.C., Bauer, S.R., Pernar, C.H., Chan, J.M., Van Blarigan, E.L., Giovannucci, E.L., Kenfield, S.A., Mucci, L.A.: Association of plant-based diet index with prostate cancer risk. Am. J. Clin. Nutr. **115**(3), 662–670 (2022) https://doi.org/10.1093/ajcn/nqab365

[9] Al-Snafi, A.: Chemical constituents and pharmacological effects of lepidium sativum. Int. J. Curr. Pharm. Res. **11**(6), 1–10 (2019) https://doi.org/10.22159/ijcpr.2019v11i6.36338

[10] Ibrahim, M.M., Mounier, M.M., Bekheet, S.A.: Targeting apoptotic anticancer response with natural glucosinolates from cell suspension culture of lepidium sativum. J. Genet. Eng. Biotechnol. **21**(1), 53 (2023) https://doi.org/10.1186/s43141-023-00511-y

[11] Taïbi, K., Abderrahim, L.A., Ferhat, K., Betta, S., Taïbi, F., Bouraada, F., Boussaid, M.: Ethnopharmacological study of natural products used for traditional cancer therapy in algeria. Saudi Pharm. J. **28**(11), 1451–1465 (2020) https://doi.org/10.1016/j.jsps.2020.09.011

[12] Banerjee, P., Eckert, A.O., Schrey, A.K., Preissner, R.: Protox-ii: A webserver for the prediction of toxicity of chemicals. Nucleic Acids Res. **46**(W1), 257–263 (2018) https://doi.org/10.1093/nar/gky318

[13] Drwal, M.N., Banerjee, P., Dunkel, M., Wettig, M.R., Preissner, R.: Protox: A web server for the in silico prediction of rodent oral toxicity. Nucleic Acids Res. **42**(W1), 53–58 (2014) https://doi.org/10.1093/nar/gku401

[14] CambridgeSoft Corporation: ChemBioDraw Ultra, version 14.0. Software (2014)

[15] Daina, A., Michielin, O., Zoete, V.: Swisstargetprediction: Updated data and new features for efficient prediction of protein targets of small molecules. Nucleic Acids Res. **47**(W1), 357–364 (2019) https://doi.org/10.1093/nar/gkz382

[16] Ferrari, I.V., De Gregorio, A., Fuggetta, M.P., Ravagnan, G.: Pharmmapper server and molecular docking study focusing on polydatin to identify potential

targets. Eur. J. Appl. Sci. **11**(5) (2023) https://doi.org/10.14738/aivp.115.15413

[17] Liu, X., Ouyang, S., Yu, B., Liu, Y., Huang, K., Gong, J., Zheng, S., Li, Z., Li, H., Jiang, H.: Pharmmapper server: A web server for potential drug target identification using pharmacophore mapping approach. Nucleic Acids Res. **38**(suppl_2), 609–614 (2010) https://doi.org/10.1093/nar/gkq300

[18] Wang, X., Shen, Y., Wang, S., Li, S., Zhang, W., Liu, X., Lai, L., Pei, J., Li, H.: Pharmmapper 2017 update: A web server for potential drug target identification with a comprehensive target pharmacophore database. Nucleic Acids Res. **45**(W1), 356–360 (2017) https://doi.org/10.1093/nar/gkx374

[19] Nickel, J., Gohlke, B.-O., Erehman, J., Banerjee, P., Rong, W.W., Goede, A., Dunkel, M., Preissner, R.: Superpred: Update on drug classification and target prediction. Nucleic Acids Res. **42**(W1), 26–31 (2014) https://doi.org/10.1093/nar/gku477

[20] Consortium, U.: Uniprot: A worldwide hub of protein knowledge. Nucleic Acids Res. **47**(D1), 506–515 (2019) https://doi.org/10.1093/nar/gky1049

[21] Zaru, R., Orchard, S., Consortium, U.: Uniprot tools: Blast, align, peptide search, and id mapping. Curr. Protoc. **3**(3), 697 (2023) https://doi.org/10.1002/cpz1.697

[22] Guzmán-Flores, J.M., Pérez-Vázquez, V., Martínez-Esquivias, F., Isiordia-Espinoza, M.A., Viveros-Paredes, J.M.: Molecular docking integrated with network pharmacology explores the therapeutic mechanism of cannabis sativa against type 2 diabetes. Curr. Issues Mol. Biol. **45**(9), 7228–7241 (2023) https://doi.org/10.3390/cimb45090457

[23] Safran, M., Dalah, I., Alexander, J., Rosen, N., Iny Stein, T., Shmoish, M., Nativ, N., Bahir, I., Doniger, T., Krug, H., *et al.*: Genecards version 3: The human gene integrator. Database **2010**, 020 (2010) https://doi.org/10.1093/database/baq020

[24] Piñero, J., Ramírez-Anguita, J.M., Saüch-Pitarch, J., Ronzano, F., Centeno, E., Sanz, F., Furlong, L.I.: The disgenet knowledge platform for disease genomics: 2019 update. Nucleic Acids Res. **48**(D1), 845–855 (2020) https://doi.org/10.1093/nar/gkz1021

[25] Davis, A.P., Grondin, C.J., Johnson, R.J., Sciaky, D., McMorran, R., Wiegers, J., Wiegers, T.C., Mattingly, C.J.: The comparative toxicogenomics database: update 2019. Nucleic Acids Res. **47**(D1), 948–954 (2019) https://doi.org/10.1093/nar/gky868

[26] Szklarczyk, D., Gable, A.L., Nastou, K.C., Lyon, D., Kirsch, R., Pyysalo, S., Doncheva, N.T., Legeay, M., Fang, T., Bork, P., *et al.*: The string database in 2021: Customizable protein–protein networks, and functional characterization of user-uploaded gene/measurement sets. Nucleic Acids Res. **49**(D1), 605–612

(2021) https://doi.org/10.1093/nar/gkaa1074

[27] Shannon, P., Markiel, A., Ozier, O., Baliga, N.S., Wang, J.T., Ramage, D., Amin, N., Schwikowski, B., Ideker, T.: Cytoscape: A software environment for integrated models of biomolecular interaction networks. Genome Res. **13**(11), 2498–2504 (2003) https://doi.org/10.1101/gr.1239303

[28] Chin, C.-H., Chen, S.-H., Wu, H.-H., Ho, C.-W., Ko, M.-T., Lin, C.-Y.: cytohubba: Identifying hub objects and sub-networks from complex interactome. BMC Syst. Biol. **8**, 11 (2014) https://doi.org/10.1186/1752-0509-8-S4-S11

[29] Huang, D.W., Sherman, B.T., Lempicki, R.A.: Systematic and integrative analysis of large gene lists using david bioinformatics resources. Nat. Protoc. **4**(1), 44–57 (2009) https://doi.org/10.1038/nprot.2008.211

[30] Chakraborty, G., Nandakumar, S., Hirani, R., Nguyen, B., Stopsack, K.H., Kreitzer, C., Rajanala, S.H., Ghale, R., Mazzu, Y.Z., Pillarsetty, N.V.K., *et al.*: The impact of pik3r1 mutations and insulin–pi3k–glycolytic pathway regulation in prostate cancer. Clin. Cancer Res. **28**(16), 3603–3617 (2022) https://doi.org/10.1158/1078-0432.CCR-21-4272

[31] Lipinski, C.A., Lombardo, F., Dominy, B.W., Feeney, P.J.: Experimental and computational approaches to estimate solubility and permeability in drug discovery and development settings. Adv. Drug Deliv. Rev. **64**, 4–17 (2012) https://doi.org/10.1016/j.addr.2012.09.019

[32] Veber, D.F., Johnson, S.R., Cheng, H.-Y., Smith, B.R., Ward, K.W., Kopple, K.D.: Molecular properties that influence the oral bioavailability of drug candidates. J. Med. Chem. **45**(12), 2615–2623 (2002) https://doi.org/10.1021/jm020017n

[33] Ghose, A.K., Viswanadhan, V.N., Wendoloski, J.J.: A knowledge-based approach in designing combinatorial or medicinal chemistry libraries for drug discovery. 1. a qualitative and quantitative characterization of known drug databases. J. Comb. Chem. **1**(1), 55–68 (1999) https://doi.org/10.1021/cc9800071

[34] Egan, W.J., Merz, K.M., Baldwin, J.J.: Prediction of drug absorption using multivariate statistics. J. Med. Chem. **43**(21), 3867–3877 (2000) https://doi.org/10.1021/jm000292e

[35] Muegge, I., Heald, S.L., Brittelli, D.: Simple selection criteria for drug-like chemical matter. J. Med. Chem. **44**(12), 1841–1846 (2001) https://doi.org/10.1021/jm015507e

[36] Ertl, P., Rohde, B., Selzer, P.: Fast calculation of molecular polar surface area as a sum of fragment-based contributions and its application to the prediction of drug transport properties. J. Med. Chem. **43**(20), 3714–3717 (2000) https:

//doi.org/10.1021/jm000942e

[37] Wildman, S.A., Crippen, G.M.: Prediction of physicochemical parameters by atomic contributions. J. Chem. Inf. Comput. Sci. **39**(5), 868–873 (1999) https://doi.org/10.1021/ci990307l

[38] Sharom, F.J.: Abc multidrug transporters: structure, function and role in chemoresistance. Pharmacogenomics **9**(1), 105–127 (2008) https://doi.org/10.2217/14622416.9.1.105

[39] Hollenberg, P.F.: Characteristics and common properties of inhibitors, inducers, and activators of cyp enzymes. Drug Metab. Rev. **34**(1–2), 17–35 (2002) https://doi.org/10.1081/DMR-120001387

[40] Huang, S.-M., Strong, J.M., Zhang, L., Reynolds, K.S., Nallani, S., Temple, R., Abraham, S., Habet, S.A., Baweja, R.K., Burckart, G.J., *et al.*: New era in drug interaction evaluation: Us food and drug administration update on cyp enzymes, transporters, and the guidance process. J. Clin. Pharmacol. **48**(6), 662–670 (2008) https://doi.org/10.1177/0091270007312153

[41] Kirchmair, J., Göller, A.H., Lang, D., Kunze, J., Testa, B., Wilson, I.D., Glen, R.C., Schneider, G.: Predicting drug metabolism: experiment and/or computation? Nat. Rev. Drug Discov. **14**(6), 387–404 (2015) https://doi.org/10.1038/nrd4581

[42] Siramshetty, V.B., Nickel, J., Omieczynski, C., Gohlke, B.-O., Drwal, M.N., Preissner, R.: Withdrawn—a resource for withdrawn and discontinued drugs. Nucleic Acids Res. **44**(D1), 1080–1086 (2016) https://doi.org/10.1093/nar/gkv1192

[43] Kroes, R., Renwick, A., Cheeseman, M., Kleiner, J., Mangelsdorf, I., Piersma, A., Schilter, B., Schlatter, J., Van Schothorst, F., Vos, J., *et al.*: Structure-based thresholds of toxicological concern (ttc): guidance for application to substances present at low levels in the diet. Food Chem. Toxicol. **42**(1), 65–83 (2004) https://doi.org/10.1016/j.fct.2003.08.006

[44] Schrey, A.K., Nickel-Seeber, J., Drwal, M.N., Zwicker, P., Schultze, N., Haertel, B., Preissner, R.: Computational prediction of immune cell cytotoxicity. Food Chem. Toxicol. **107**, 150–166 (2017) https://doi.org/10.1016/j.fct.2017.05.041

[45] Ames, B.N., Durston, W.E., Yamasaki, E., Lee, F.D.: Carcinogens are mutagens: a simple test system combining liver homogenates for activation and bacteria for detection. Proc. Natl. Acad. Sci. U.S.A. **70**(8), 2281–2285 (1973) https://doi.org/10.1073/pnas.70.8.2281

[46] Freshney, R.I.: Culture of Animal Cells: A Manual of Basic Technique and Specialized Applications. John Wiley & Sons, ??? (2015). Edition and place of publication

not provided

Supplementary Files

This is a list of supplementary files associated with this preprint. Click to download.

- SupplementaryFile.xlsx